

Article

Trend in Extreme Precipitation Indices Based on Long Term In Situ Precipitation Records over Pakistan

Asher Samuel Bhatti ^{1,2}, Guojie Wang ^{1,*} , Waheed Ullah ¹ , Safi Ullah ³ ,
Daniel Fiifi Tawia Hagan ¹ , Isaac Kwesi Nooni ^{1,4} , Dan Lou ¹ and Irfan Ullah ³ 

¹ Collaborative Innovation Center on Forecast and Evaluation of Meteorological Disasters, School of Geographical Sciences, Nanjing University of Information Science and Technology (NUIST), Nanjing 210044, China; asher.samuel@nuist.edu.cn (A.S.B.); waheed.wama@nuist.edu.cn (W.U.); dans7messiah@nuist.edu.cn (D.F.T.H.); nooni25593@alumni.itc.nl (I.K.N.); loudan711@163.com (D.L.)

² Department of Geology, Bacha Khan University Charsadda, Khyber Pakhtunkhwa Pakistan, P.O. Box 20, Charsadda 24420, Pakistan

³ School of Atmospheric Sciences, Nanjing University of Information Science & Technology, Nanjing 210044, China; safikhalil442@yahoo.com (S.U.); irfanullahparas92@yahoo.com (I.U.)

⁴ Binjiang College, Nanjing University of Information Science & Technology, No.333 Xishan Road, Wuxi 214105, Jiangsu Province, China

* Correspondence: gwang@nuist.edu.cn

Received: 31 January 2020; Accepted: 9 March 2020; Published: 12 March 2020



Abstract: Assessing the long-term precipitation changes is of utmost importance for understanding the impact of climate change. This study investigated the variability of extreme precipitation events over Pakistan on the basis of daily precipitation data from 51 weather stations from 1980–2016. The non-parametric Mann–Kendall, Sen’s slope estimator, least squares method, and two-tailed simple *t*-test methods were used to assess the trend in eight precipitation extreme indices. These indices were wet days ($R1 \geq 1$ mm), heavy precipitation days ($R10 \geq 10$ mm), very heavy precipitation days ($R20 \geq 20$ mm), severe precipitation ($R50 \geq 50$ mm), very wet days ($R95p$) defining daily precipitation ≥ 95 percentile, extremely wet days ($R99p$) defining daily precipitation ≥ 99 percentile, annual total precipitation in wet days (PRCPTOT), and mean precipitation amount on wet days as simple daily intensity index (SDII). The study is unique in terms of using high stations’ density, extended temporal coverage, advanced statistical techniques, and additional extreme indices. Furthermore, this study is the first of its kind to detect abrupt changes in the temporal trend of precipitation extremes over Pakistan. The results showed that the spatial distribution of trends in different precipitation extreme indices over the study region increased as a whole; however, the monsoon and westerlies humid regions experienced a decreasing trend of extreme precipitation indices during the study period. The results of the sequential Mann–Kendall (SqMK) test showed that all precipitation extremes exhibited abrupt dynamic changes in temporal trend during the study period; however, the most frequent mutation points with increasing tendency were observed during 2011 and onward. The results further illustrated that the linear trend of all extreme indices showed an increasing tendency from 1980–2016. Similarly, for elevation, most of the precipitation extremes showed an inverse relationship, suggesting a decrease of precipitation along the latitudinal extent of the country. The spatiotemporal variations in precipitation extremes give a possible indication of the ongoing phenomena of climate change and variability that modified the precipitation regime of Pakistan. On the basis of the current findings, the study recommends that future studies focus on underlying physical and natural drivers of precipitation variability over the study region.

Keywords: extreme precipitation indices; Pakistan; Mann–Kendall; Sen’s slope estimator

1. Introduction

The Intergovernmental Panel on Climate Change (IPCC) stated in its Fifth Assessment Report (AR5) that global warming-induced climate change has affected the frequency, intensity, and duration of extreme precipitation (P) events in both space and time [1,2]. These variations in P extremes result in floods, droughts, and heatwaves [3–5], which have serious health, social, economic, and environmental implications on millions of people and on ecosystems across the globe [6–8]. However, the severity, duration, and geographical extent of these extreme events and their impacts vary from region to region [9,10]. In recent studies, it has been reported that the changes detected in P extremes during the late 20th century are projected to continue into the future with even more severe impacts [11–13]. Due to the current and future intensification, the study of P extremes has gained significant attention among climate scientists in recent times [14,15]. The robust trend analysis of historical P extremes plays a key role in regional climate assessment, water resource management, and sustainable agricultural practices [16,17]. Moreover, the information obtained from such analysis is crucial in devising a compressive plan for future climate change adaptation and mitigation strategies at regional and local scales [18,19].

Several research studies have been conducted to assess the spatiotemporal trends in P extremes in different regions of the world. Most of these studies reported positive trends in P extremes [20–22]; however, a high spatiotemporal variability exists in the frequency and intensity of extreme P events over different climatological regions of the world [1]. In recent studies, an increasing trend has been reported in P extremes over the Tibetan Plateau [20,23,24], South Asia [25–27], Central Asia [28–30], Europe [31,32], and the Arab region [33,34]. In addition, the frequency and intensity of extreme P events have shown an increasing trend in mainland China over the last few decades [35–38]. Similarly, the increasing trend of P extremes has been reported over Bangladesh in recent years [39–41]. In addition, Deshpande et al. [42] reported a positive trend in extreme P events in India during the period of 1951–2013. The findings of the aforementioned studies indicate that climate change has intensified spatiotemporal variability of P extremes over different regions of the world.

Pakistan is one of the countries highly vulnerable to climate change due to its complex topography, geographical location, dynamic climatology, and low coping capacity [27,43]. Similar to global patterns, climate change has significantly affected the spatiotemporal variability of P extremes in Pakistan [44–46]. According to the worldwide climate risk index, Pakistan is among the top 10 countries affected by climate change [1,47]. Recently, many studies have reported dynamic changes in extreme P events over different parts of Pakistan [25,27,48–52]. The spatiotemporal variability of P extremes has imbalanced the availability of water resources and caused several hydro-meteorological disasters in the country [53,54]. The recent floods (of 2010) and prolonged drought (of 1997–2002) bear witness to climate change-induced extremes, which have affected millions of people across the country [18,55–57]. Thus, more research is needed to assess the magnitude of the changes for a better understanding of the regional scale impact of climate change.

As a developing country, Pakistan needs advanced knowledge, innovative ideas, and a better understanding of the P extremes and their effects on our ecosystem and different sectors of the society [19,58]. Therefore, it is critical to assess the long-term spatiotemporal variations in P extremes and proposed useful recommendations for climate change adaptation and disaster risk reduction in the region. The objective of this study was to determine the spatial and temporal changes in extreme P events in Pakistan from 1980 to 2016. The novelty of this study is its use of high stations' density, extended temporal coverage, advanced statistical techniques, and additional extreme indices. Furthermore, this study is the first of its kind to detect abrupt changes in the temporal trend of precipitation extremes over the target region.

The remainder of the paper is organized as follows. In Section 2, we briefly describe the study area as well as the data and methods. Section 3 presents the results for the study. The discussion and conclusions are summarized in Sections 4 and 5, respectively.

2. Study Area

Pakistan is located in a sub-tropical to tropical region with a latitudinal span of 23°N to 37°N and a longitudinal span of 61°E to 78°E (Figure 1). The elevation of the country varies from a few meters in the south to over 6000 meters in the north [46,59]. The country exhibits a multifaceted landscape with elevated mountains in the upper reach, flat agricultural land in middle reach, and the coastal belt in the lower reach (see Figure 1) [43,60]. The hydrological cycle of the country varies along with the latitudinal extent with minimum P in the lower reach (<150 mm) and maximum in the upper reach (>500mm) annually [61,62]. In terms of temperature (T) distribution, the maximum average T (>35°C) is found in the lower reach, whereas the upper reach records a minimum average T (<0°C) [43,59,63]. The dominant P seasons of the region are monsoon and westerlies, which occur during summer and winter seasons, altogether driving the local hydrological cycle [46,61]. The recent warming hiatus of the globe appeared to be impacting the hydrometeorological cycle of Pakistan [27,64], with apparent changes in P [46,65].

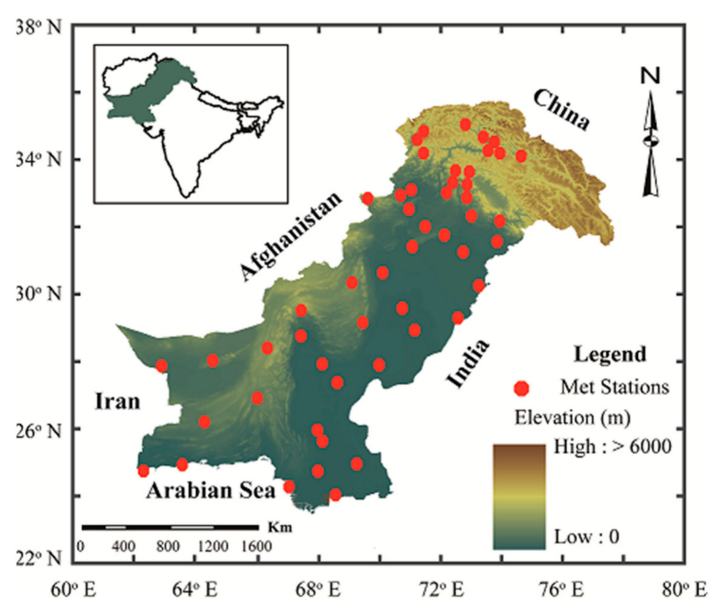


Figure 1. Map of the study area showing political boundary of Pakistan with altitude and selected stations.

3. Data and Methods

3.1. Data

To document changes in extreme P events during 1980–2016, the daily P records of 51 stations were obtained from the Pakistan Meteorological Department (PMD) (Figure 1). The PMD operates a dense network of synoptic-scale weather stations across the country to monitor different hydrometeorological variables for their proper use and related studies [63]. To ensure quality of the datasets, extensive visual and numeric checks for any missing and homogeneity issues were conducted [66]. The commonly used approaches for homogeneity testing such as the standardized normal homogeneity test (SNHT) was adopted [59]. The homogenization practice intended to detect outliers or spikes in the observation dataset, as well as in the instrumentations, relocations, replacements, environment, and procedures during the data collection process, caused after unavoidable errors [36,63]. This test has been widely used by different researchers in hydrometeorological studies [14,59,67–69]. We found only a small amount of data (<3%) were missing in a few stations, which may not have influenced the results of the study to a greater extent. The datasets were further processed to estimate the regional scale and station scale P climatology at seasonal and annual timescale.

3.2. Precipitation Indices

In this study, we used six indices from the list of the Experts Team on Climate Change Detection Indices (ETCCDI) of the World Meteorological Organization (WMO) [70,71]. The details of the selected indices are presented in Table 1. These indices were suitable to assess and quantify the impacts of climate change over Pakistan. Moreover, the evaluation of indices can provide solid evidence of the current and future climate change in the country.

Table 1. List of selected precipitation indices.

Name	ID	Definition
Wet days	R1 mm	Annual count of days when precipitation ≥ 1 mm
Heavy precipitation days	R10 mm	Annual count of days when precipitation ≥ 10 mm
Very heavy precipitation days	R20 mm	Annual count of days when precipitation ≥ 20 mm
Severe precipitation days	R50 mm	Annual count of days when precipitation ≥ 50 mm
Annual total precipitation	PRCPTOT	Annual total precipitation in wet days
Simple daily intensity index	SDII	Mean precipitation amount on wet days
Very wet days	R95p	Annual precipitation ≥ 95 percentile
Extremely wet days	R99p	Annual precipitation ≥ 99 percentile

3.3. Statistical Techniques

To assess the spatiotemporal changes' precipitation extremes over Pakistan, this study used different statistical approaches: Mann–Kendall (MK), Sen's slope (SS) estimator, linear regression, and Student's *t*-test. The non-parametric MK test was used to determine significant trends in precipitation indices [72,73], whereas the SS estimator was employed to calculate the magnitude of the trend in the selected indices [74]. To detect abrupt changes or shifts in the temporal trend of precipitation indices, we used the non-parametric sequential Mann–Kendall (SqMK) test. Moreover, linear regression and two tailed Student's *t*-test were used to detect the significant linear trends in the precipitation indices over the study region [75,76]. The selected statistical techniques have been widely used by various researchers in their climatological and hydrological studies over different climatic regions of the world [18,52,77–81]. These statistical tests are briefly discussed in the following sections.

3.3.1. Mann–Kendall (MK) Test

The MK test was applied to determine the significance test in time series of precipitation indices. The test does not require normal distribution of data and does not depend on the space–time of monitoring and the magnitude of data missing values. The following mathematical expression of a standardized MK trend statistic (Equation (1)) was used to generate a significance test of the monotonic trend, which was based on the Kendall rank correlation:

$$S = \sum_{k=1}^{m-1} \sum_{l=k+1}^m \text{sig}(x_l - x_k) \quad (1)$$

where $\text{Sig}(x_l \text{ and } x_k)$ can be computed by Equation (2):

$$\text{sig}(x_l - x_k) = \begin{cases} 1 & x_l > x_k \\ 0 & x_l = x_k \\ -1 & x_l < x_k \end{cases} \quad (2)$$

where x_l and x_k are the data points of the time series and m is the data length of the time-series. In detecting the trend, a hypothesis was set as follows: null hypothesis (H_0) signified no trend, and

the alternative hypothesis (H_1) indicated the presence of a trend, either an increasing or decreasing monotonic trend. The variance of S was calculated using Equation (3):

$$\text{Variance}(S) = \frac{m(m-1)(2m+5)}{18} \quad (3)$$

The probability associated with S and the sample size, n , was calculated to assess the significance of the trend. The significance of the trend was determined using a Z value, where a negative (positive) score of Z denotes a downward (upward) trend. For a two-tailed test, at a given α (0.05) level of significance, H_1 is accepted if the $|Z| > Z_{1-\alpha/2}$, where $Z_{1-\alpha/2}$ is tabulated from the standard normal distribution tables. The probability associated with MK and sample size n was computed to statistically quantify the significance of the trend. The normalized test statistic, Z , was calculated using Equation (4):

$$Z = \begin{cases} \frac{S-1}{\sqrt{\text{Variance}(S)}} & \text{if } S > 0 \\ 0 & \text{if } S < 0 \\ \frac{S+1}{\sqrt{\text{Variance}(S)}} & \text{if } S < 0 \end{cases} \quad (4)$$

The trend is considered decreasing if Z is negative and computed probability is greater than the level of significance. This methodology has been successfully employed in many related studies thus far [63,82,83].

3.3.2. Sen's Slope Estimator

The nonparametric Sen's slope estimator (Sen 1968) test was used to estimate the magnitude of trends, which assumes that the trend is linear. When a linear trend exists in a time series, then the slope (Q_i) of a time series can be expressed as $X = x_j - x_k$ and $N = j - k$ if $j > k$, and calculated as

$$Q_i = \frac{X}{Y} \text{ for } i = 1, 2, 3 \dots n \quad (5)$$

where X represent the difference of annual values.

3.3.3. Sequential Mann-Kendall (SqMK) Test

The SqMK test was introduced by [84] to determine the significant mutation points in a time series. The abrupt changes in the temporal trend are estimated by the series of the forward sequential statistic (u_t) and backward sequential statistic (u'_t). The sequential behaviors of u_t fluctuate around the zero, as it is a standardized variable with zero mean and unit standard deviation. Moreover, it has the same nature as that of Z values, starting from the first to last data point. On the other hand, the value of u'_t is computed backward, starting from the endpoint to the first point of a time series. The test considers relative values of all terms in a time series (x_1, x_2, \dots, x_n). The following steps can express the test.

Firstly, the magnitudes of x_j annual mean time series ($j = 1, \dots, n$) and x_k ($k = 1, \dots, j-1$) are compared. The number of cases $x_j > x_k$ is counted, and n_j denotes the outcome.

The test statistic t is computed by Equation (6):

$$t_j = \sum_1^j n_j \quad (6)$$

The mean and variance of the t are calculated by Equations (7) and (8), respectively:

$$E(t) = [n(n-1)]/4 \quad (7)$$

$$\text{Var}(t_j) = j(j-1)(2j+5)/72 \quad (8)$$

At the end, the sequential values of u_t and u'_t are calculated by Equation (9):

$$u_t(t) = [t_j E(t)] / \sqrt{\text{var}(t_j)} \quad (9)$$

If $|u_t(t)| \leq u_t(t)_{1-\alpha/2}$, where $u_t(t)_{1-\alpha/2}$ is the critical value of the standard normal distribution with a probability value exceeding $\alpha/2$, the null hypothesis would be accepted at a significance level in the trend test. In this study, we set the α value as 0.05. The decreasing values of u_t and u'_t indicate a negative trend, whereas the increasing values represent a positive trend in the time series. The intersection points of u_t and u'_t curves indicate the possible turning year of the trend within a time. The trend turning point is considered significant at the corresponding threshold level (i.e., ± 1.96 for 95% significance level).

4. Results

4.1. Long-Term Climatology of Pakistan

The precipitation (P) variability of the region is shown in Figure 2, indicating the long-term mean precipitation at station scale (Figure 2a), and mean monthly P averaged for the whole stations (Figure 2b) in the study region. From Figure 2a, the annual mean P pattern appeared to be following a distinct latitudinal variation from south to northwards. In the upper reach (i.e., northern humid region), the annual mean P ranged from >30 mm to >150 mm. The region was located in the foothills of the Himalayan Mountains, and is the core monsoon region. Moreover, the region also received an adequate amount of seasonal P from the westerlies system. However, the extreme northern parts appeared to show a decrease in annual mean (1.0 to 30mm) due to their geographical location, where only westerlies were the primary source of local scale hydrological cycle [62]. Similarly, the lower reach (i.e., southern parts) were characterized by arid and semi-arid climates with minimal quantity of precipitation (<30 mm). It should be noted that the southern parts of Pakistan are dominated by the coastal and tropical climate and are isolated from the monsoon and westerlies systems [46,59].

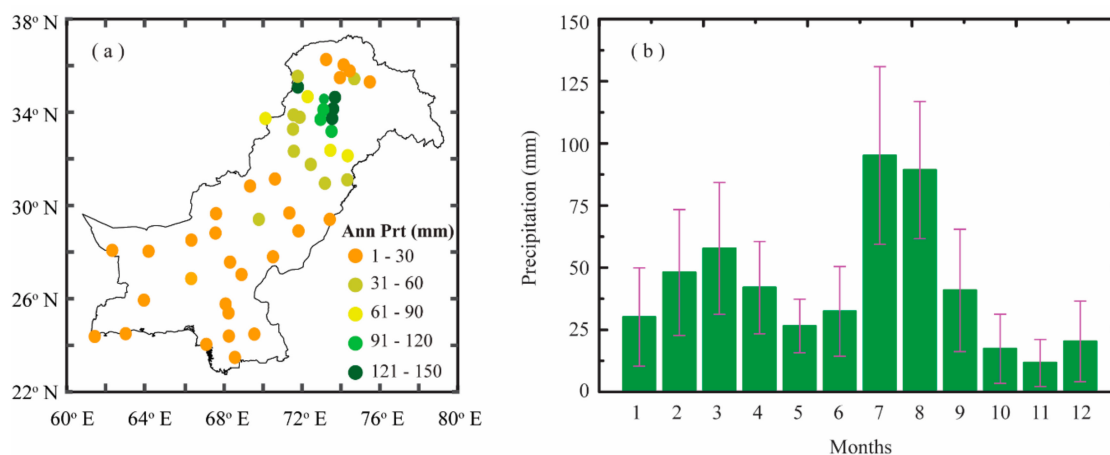


Figure 2. Spatial map of (a) climatological mean annual precipitation and (b) mean monthly precipitation during 1980–2016.

From Figure 2b, clear P seasonality can be seen with two modes of P : one during winter months, pre-monsoon due to western P system, and one during summer months due to the monsoon system. The two modes of P were locally driving the hydrological cycle by maintaining the perennial flow in the Indus basin river system. The peak P months during westerlies were found to be February, March, and April, whereas July and August were found as the peak P months during monsoon season. Altogether, these two P patterns are responsible for supporting the local water supply, agricultural production, and hydropower generation. The latitudinal variability added the benefit of holding all

precipitating water inside the country. However, excess/deficit of these two P systems also appeared to be affecting the region adversely [46,52].

4.2. The Trend in Extreme Precipitation Indices

Figure 3 shows the spatial distribution of trend in different P indices, as described in the Methods section. From Figure 3a, it can be seen that the number of rainy days ($P \geq 1$ mm) increased (0.40 days) in the study region. The increase was more evident in the eastern and northern parts, whereas the southwestern arid and central humid regions showed a decrease (-0.39 days) during the study period. The analysis further illustrated that the heavy precipitating days with a magnitude of ≥ 10 mm showed a significant decrease (Figure 3b) in humid and northern semi-arid regions of the country (-0.25 days). It was interesting to see an increasing trend of > 0.2 days in the heavy P in the central and eastern parts of the country, whereas there was a decrease of < -0.2 days in the southern and southwestern regions.

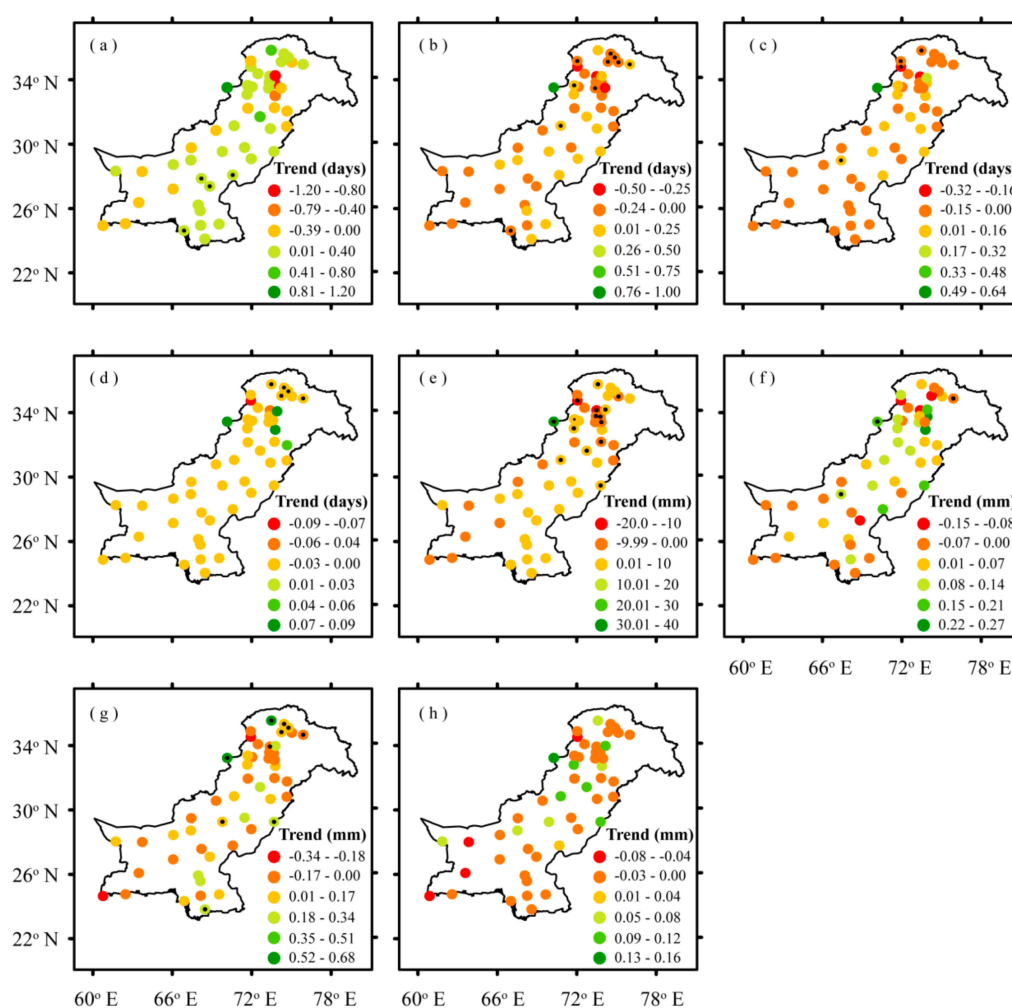


Figure 3. Spatial distribution of trend in different precipitation (P) indices over the study region: (a) R1 ≥ 1 mm, (b) R10 ≥ 10 mm, (c) R20 ≥ 20 mm, (d) R50 ≥ 50 mm, (e) annual total precipitation in wet days (PRCPTOT), (f) simple daily intensity index (SDII), (g) very wet days (R95p), and (h) extremely wet days (R99p). The black dots in the colored circles indicate a significant trend at the 0.05 significance level.

An asymmetric pattern can be seen for the very heavy precipitating days with a magnitude ≥ 20 mm (Figure 3c) in the region with a decrease (increase) in the northern and southern (central) regions of the country at the rate of -0.2 days (0.25 days). For severe P days ($P \geq 50$ mm), except for a few stations in the humid region (see Figure 3d), the remainder of the country showed a slight

decline with < -0.03 days during the study period. The annual total P (Figure 3e) exhibited an overall increasing trend of > 0.01 mm in the eastern and northern parts of the study region.

Few stations in the humid and semi-arid core monsoon region of the country and southwestern coastal part exhibited a decreasing trend of < -9.9 mm during 1980–2016. The magnitude of mean P (Figure 3f) showed an overall increase of > 0.14 mm in monsoon P regions of the country, whereas a decrease can be seen in the northern and southern arid regions (< -0.1 mm) of the country. The humid, and high-altitude regions of the country in the north appeared to be under decreasing P (< -0.17 mm) with 95th percentile (Figure 3g), whereas an increase of > 0.015 mm can be seen in the eastern and southeastern parts of the country. The 99th percentile P (Figure 3h) appeared to be decreasing at the rate of < -0.08 mm over the southwestern coastal and northern regions of the country. At the same time, an increase of > 0.06 mm was reported in the 99th percentile over the central and western parts of the country.

From Figure 3, it can be concluded that the P as a whole appeared to be increasing in the study region; however, there were certain modes for each index. The central arid regions experienced a rise in P magnitude, events, and frequency during the study period. It was noteworthy that the extreme P magnitude appeared to be least affected with an increasing marginal trend of the 95th and 99th percentile P events. The findings were rather interesting to see, as the core monsoon and westerlies humid regions were drying due to a decrease in P indices, whereas the southern and western parts exhibited an increasing trend, suggesting a potential shift in the monsoon maxima from the humid regions towards the western arid regions of the country.

At the same time, the indices experienced an increase in the general monsoon domain, suggesting a possible expansion in the monsoon span over the study region; however, the impact of westerlies should also be considered, which have been increased over the recent past. The increasing trend could suggest more extreme events can induce potential risks in the form of riverine floods, flash floods, and drought over different parts of the country. The dynamic variability of these extremes can increase the degree of exposure and vulnerability of the communities living in the downstream regions of the Indus River Basin. The overall results appeared to be similar to those of [48,85], who reported comparable findings.

Figure 4 shows the SqMK test statistics in the time domain for the selected P indices over the region. The results inferred that rainy days (R1 mm) followed a decreasing trend (Figure 4a) in the early 1980s, followed by a distinct increase (decrease) in early 1990 (2000) and a smooth increase later on from 2011 onward. The heavy (Figure 4b), very heavy (Figure 4c), severe P events (Figure 4d), and annual total P (Figure 4e) appeared to be following the same pattern with an evident decrease (increase) in 1980 (1990). The trend seemed to be smoothly increasing after 2005, inferring an increased frequency of extreme P events in the study region. The systematic increase/decrease in extreme precipitation in terms of magnitude coincides with the wet/dry events observed in the study region [46,85], possibly induced by anomalous large-scale circulation or oceanic indices and thus requires further exploration [55,86–88]. The increase in these events at the later part of the study further suggests that the footprints of climate change-induced variability in water cycle are obvious at a regional scale and thus may enhance the frequency of flooding events as observed over the past years [47,57]. The mean P on wet days (Figure 4f) exhibited a small variability until 2000, and a significant smooth drop can be seen during early 2000, followed by a significant increase for the rest of the study duration. The 95th percentile P events (Figure 4g) exhibited a decreasing trend, which was significant in the recent decade around 2012 and continued to decrease later on. The 99th percentile P events (Figure 4h) appeared to be varying on a small scale over the study duration; however, a more prominent decrease can be seen at the end of the study duration, suggesting a decrease in extreme P events.

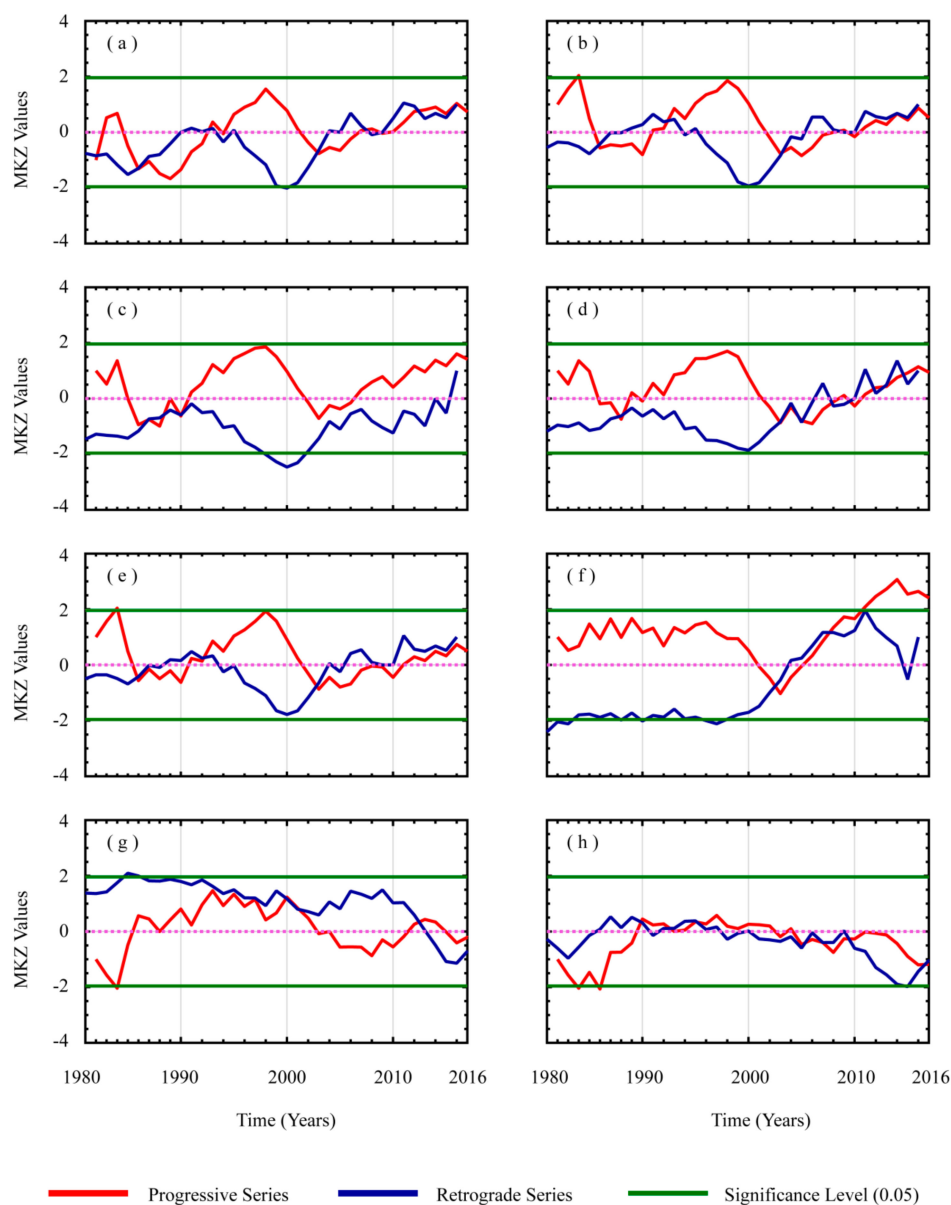


Figure 4. Sequential Mann–Kendal (SqMK) trend in different precipitation indices used in the study: (a) $R1 \geq 1$ mm, (b) $R10 \geq 10$ mm, (c) $R20 \geq 20$ mm, (d) $R50 \geq 50$ mm, (e) PRCPTOT, (f) SDII, (g) R95p, and (h) R99p.

Overall, Figure 4 can be summarized as the P indices exhibited an obvious increasing trend, especially during recent years. The turning points suggested that during the study duration, certain shifts (increase/decrease) occurred in P indices. The extreme P (95th) events appeared to be decreasing in recent years, whereas the severe events (99th) underwent a slight decrease during recent years. The study findings for the P-based magnitude and frequency are in line with those of [46,51] in the context of global climate change. For the last two indices, it is noteworthy to mention that the decreasing shift could have been due to the area average rather than the regional average, and thus some regions might have experienced an increasing/decreasing trend. However, the area averaging statistics might have suppressed the dominant signal [46]. The regional and large-scale drivers of these precipitation events can possibly be linked to those of monsoon and westerlies precipitation that occurs during the summer and winter seasons, respectively. Recent studies have reported an obvious increase in these precipitation patterns [44,46,59]. The reported increase is generally attributed

to enhanced frequency and intensity of extreme precipitation events, which are usually followed by heavy flooding events in the study region [56,57]. Such events have a long history over Pakistan, and have resulted in huge losses of agricultural lands, civil and hydrological structures, and human lives [20,47]. The data uncertainty is another limitation because the station data is usually subjected to synoptic-scale application, and recording skills are also presently subjected to deviations and thus can be acknowledged in this study [59,89]. Thus, a detail examination using advanced methods, simulations, and projections could be the alternative approach to better understand such precipitation behaviors at a regional scale [61,85].

Figure 5 shows the linear regression of the different precipitation indices used in the study. The green line shows the P indices, the dashed blue line shows 5-year moving average, and the red line shows the regression line/best-fit line. For rainy days (Figure 5a), the overall trend appeared to be increasing with the slope/regression coefficient of 0.059; however, a sharp variability during the study duration was distinct with peaks/troughs suggesting the wet/dry events of the region. The heavy (Figure 5b), very heavy (Figure 5c), and severe precipitation events (Figure 5d) appeared to be following similar patterns, as observed for daily rainy days, with an increasing trend and regression magnitudes of 0.017, 0.027, and 0.005, respectively. This increasing trend of precipitation events can be interpreted with emphasis on agriculture and thus may boost the crop and vegetation output of the study region, which is mostly comprised of arid and semi-regions with sparse vegetation. However, the heavy, very heavy, and severe precipitation events can further expose the livelihood of the community, which are already vulnerable to flood hazards. The indirect impact of these events can further also be felt in the downstream areas of the Indus basin with direct physical losses and indirect losses through waterlogging, land degradation, and deposition of transported sediments [53,56].

The temporal variability of these indices (Figure 5b–d) showed a peak in the early 1990s, followed by a decrease during 2000–2005 and then a constant increase during the later years. The annual total P (Figure 5e) and wet days mean P (Figure 5f) also increased with regression coefficients of 0.62 and 0.054, respectively. However, the increase in total P was higher as compared to mean wet days P, inferring more P magnitude on annual scale attributed to extreme events. The extreme P percentiles exhibited an increasing trend with regression coefficients of 0.046 and 0.019 for 95th and 99th percentile P events, respectively (Figure 5g,h). The dry conditions of the later 1990s and early 2000s was evident in all indices, especially in the extreme indices of 95th and 99th percentiles.

From the results of Figure 5, it can be inferred that the overall frequency and magnitude of precipitation extremes were continuously increasing during the study period. The highest increase can be seen for mean annual total precipitation on wet days. The results of linear regression were different from the SqMK trend test, where a decline in some indices was noticeable. On the contrary, an increase in the extreme indices, especially after 2000, inferred more extreme events to occur over the study region. The drought event was evident in all indices and could potentially be the reason for different statistical outputs, as observed in previous sections.

In summary, the increase in the recent years in all indices was noticeable and thus needs to be considered for regional-scale decision making such as those involving floods, food security, disaster risk, and vulnerability at a regional scale. The underlying dynamics associated with these changes in extreme precipitation events could possibly be large-scale atmospheric and oceanic factors that have been studied in similar studies over the region [57,86,88]. The findings are in line with the recent trend induced by global warming, as depicted in the IPCC recent assessment report [1,46,59,85].

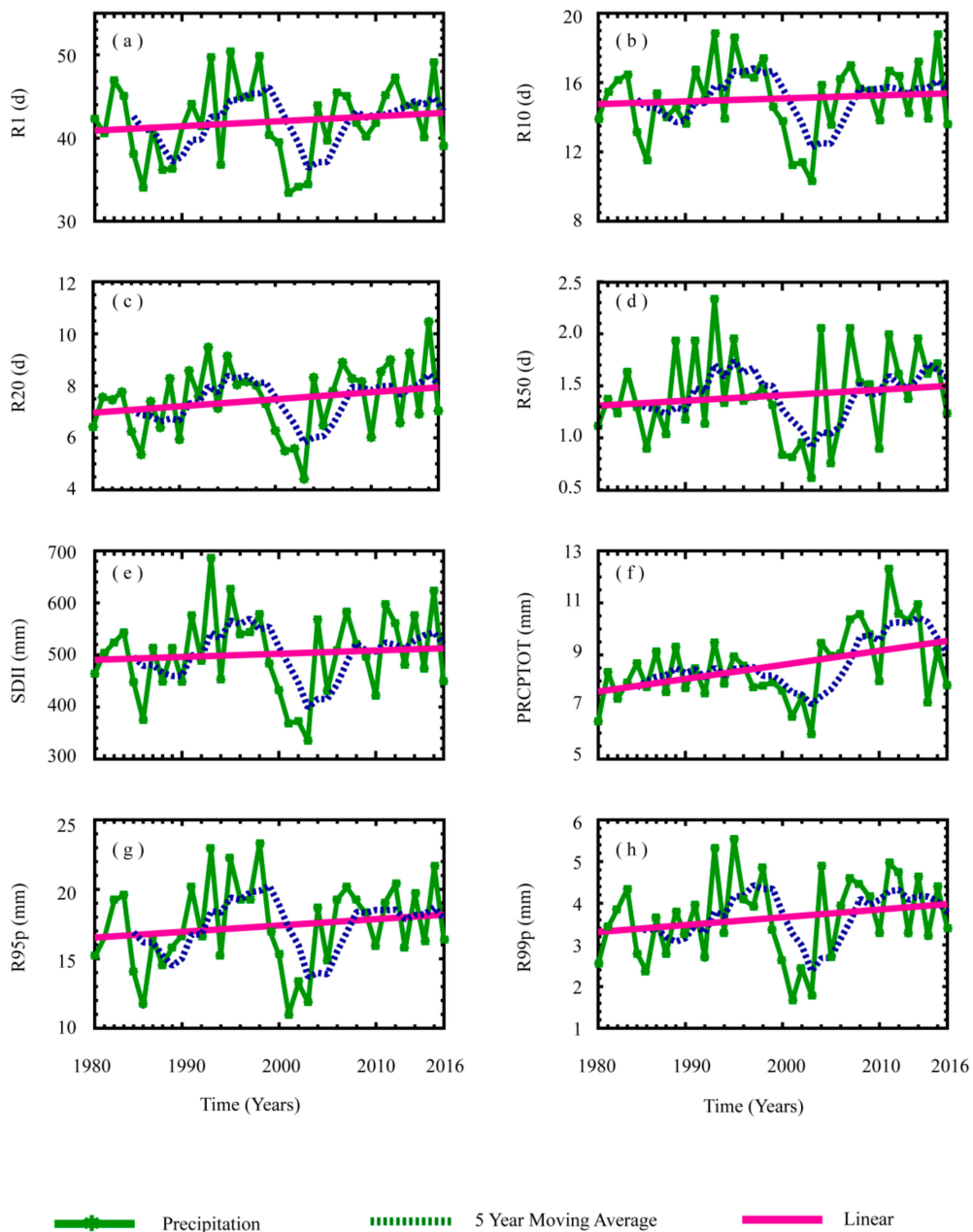


Figure 5. Linear trend in different P indices during the study period: (a) $R1 \geq 1$ mm, (b) $R10 \geq 10$ mm, (c) $R20 \geq 20$ mm, (d) $R50 \geq 50$ mm, (e) PRCPTOT, (f) SDII, (g) R95p, and (h) R99p.

Figure 6 shows the linear trend estimated for extreme precipitation indices versus the altitude of the study region. It should be noted that the study region experiences high variation in P along the latitude, thus it can also be termed as a latitudinal variation. The results suggest that wet days were slightly increasing along with the altitude (Figure 6a), inferring an increase in P from the south towards the north. Usually, the central and eastern parts of the study region experience two dominant precipitation patterns during winter, associated with western disturbances and South Asian monsoon precipitation [59,62,90]. An increasing trend in precipitation along the latitude/altitude suggests that northern and western parts of the study region are becoming relatively wetter than the rest of the region [44,46]. This can be associated with an increase in westerlies and monsoon precipitation altogether, and thus further studies to explore this pattern in more detail are required for this region, which serves as the source of water supply for the perennial river flow into the downstream parts of Indus basin. For heavy and very heavy P events (Figure 6b,c), a slight decrease in the magnitude along

altitude is obvious, suggesting an increase in the heavy P events in plane arid/semi-arid valleys and decrease in the upper humid/arid high-altitude regions. The severe P events (Figure 6d) appeared to be decreasing along with the altitude; however, in the mid-altitude monsoon regions, some stations have shown an increasing pattern. This infers that the monsoon core regions might be susceptible to these changes on a more higher pace than other parts of the region, as the eastern and southeastern regions usually receive >60% of its precipitation during monsoon season.

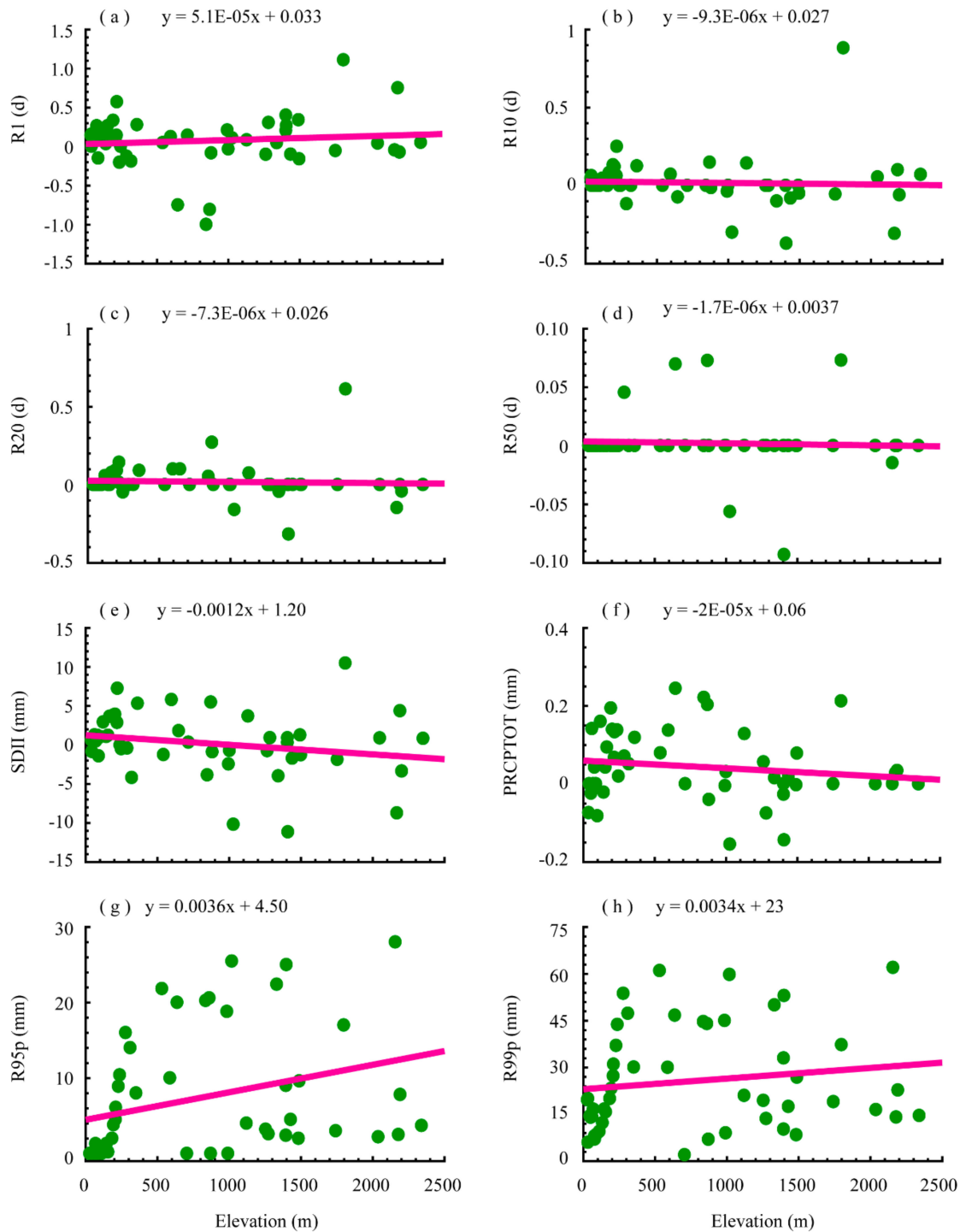


Figure 6. Linear trend in different P indices with respect to elevation used in the study: (a) $R1 \geq 1$ mm, (b) $R10 \geq 10$ mm, (c) $R20 \geq 20$ mm, (d) $R50 \geq 50$ mm, (e) PRCPTOT, (f) SDII, (g) $R95p$, and (h) $R99p$.

The overall severe P events appeared to be decreasing from southern arid/semi-arid regions towards the northern parts of the region. The daily wet days mean P (Figure 6e) and annual total P (Figure 6f) showed a slight decrease, along with the altitude with an initial increase and then decrease in the high-altitude regions. The extreme P percentile, i.e., 95th and 99th (Figure 6g,h), also exhibited an increase along the latitude, with an initial increase in coastal low altitude regions and a decrease in the central arid valley and a smooth increase in remainder of the region.

The findings of Figure 6 explain a decrease in P frequency from the south towards the north, inferring a decrease (increase) in these events in northern (southern) parts of the country, as can be seen from previous findings reported by [46,61]. For extreme P events, an increase can be seen from the south towards the north, suggesting that the region has experienced an increase in the P extreme events towards northern parts of the country. At the same time, the frequency of heavy and severe P increased in the arid southern parts of the country. The findings of the study are in line with the recent global warming trend in the region and associated changes projected by IPCC in AR5 [1,59,85]. A change in the local hydrological cycle is expected, which needs to be considered for future planning of water resources in the region [19,43,54]; however, more detailed studies can further explore such patterns in more particular ways.

5. Discussion and Conclusions

Extreme P events have increased in recent years and are projected to increase in the near future. The frequent and intense P extremes can increase the associated risk and vulnerability in terms of a riverine flood or flash flood, due to which susceptible regions are expected to be exposed exponentially across the globe. Pakistan is among the topmost vulnerable regions [4,47] due to climate change-induced P extremes, and its local hydrological cycle has been significantly affected in recent years. Moreover, it is expected that the diversity in seasonal P along the latitude/longitude and perennial flow pattern have strongly influenced the local and remote scale fauna and flora in the study region. Due to these constraints and vulnerabilities, the current study was framed to assess changes in extreme P events on the basis of selected extreme indices over the target region during 1980–2016.

The results inferred that the seasonal P is attributable to two dominant modes: westerlies in winter and pre-monsoon and monsoon seasons. The climatology inferred a consistent increase in P from the south towards the north that follows latitudinal P variability, and from the west towards east along the longitudes. On a seasonal scale, the two peak precipitating seasons are winter (January–April) that results in snowfall in northern mountains and summer monsoon season (June–September); together, these two systems drive the local water cycle of the country [59]. The increasing trend in total annual wet days (R1mm), R10mm, and R20mm infer an increase in the wet days and magnitude of precipitation. This could be associated with an increase in air T, which enhances the water holding capacity of the air and results in more water vapor in the air. The water holding capacity of the atmosphere has increased by 7% due to changes in global T, which, as stated by [65], can explain the result of more P events. P events with a magnitude of 50mm showed a slight decrease in some parts of the country, but overall the decrease was not so obvious, except for in the northern parts of the country.

PRCTOT and SDII both appeared to be increasing in the majority of the stations; the temporal evolution of the trend for both indices showed the peak wetting and drying pattern of the region. Apart from the increasing temperature in the study region [43], the large scale global warming and increased sea surface temperature could also affect the reasons for an increasing trend in these indices. Such mixed behaviors could be due to the geographical location of the region because Pakistan marks the boundary of their influence [59,89] for both precipitating seasons, and thus no distinct pattern can be seen throughout the region. For the rest of the P indices, the increase in the central Indus basin and decrease in the monsoon central and core western disturbance regions was found to be significant, except for the 99th percentile. A possible explanation could be attributed to two different aspects of the region that include the aridity of the region and moisture sources of the P for both P modes in the region.

The aridity classes of the region are mostly comprised of arid to semi-arid and extremely arid [59,91]. The occurrence of P mainly results in more infiltration and less runoff. With less runoff, the amount of evaporation and moisture recycling through evapotranspiration is limited, and hence less water is recycled through convective activities [86]. The second aspect can be explained through moisture location for both P modes that drive the regional water cycle. The shift in trend could be attributed to possible trajectory shift in the monsoon and westerlies disturbances circulations [90,92,93]. The moisture source for the summer season is over the Indian Ocean, whereas for winter it is over the Mediterranean region; the shift in the trajectory of the circulation patterns can relocate the P maxima and thus affect changes in P.

The variability in the climatology of the extreme P indices further suggests that the region experienced an increase in the extreme events during early 1990, followed by a drought event during 2000 and vice versa. The increase in extreme precipitation indices have shown an overall increase in precipitation in recent years. This increase in precipitation can impact the shifting of center of maxima and intensity of extreme precipitation events. Thus, the changes observed may alter the patterns of extreme weather events, especially flash and riverine floods in the target regions with high vulnerability to natural hazards [20,53,81]. The arid/semi-arid region in southern Pakistan, where the extreme precipitation events are decreasing, can play a major role in defining droughts. However, precipitation is not the only factor for weather and drought estimation/prediction, as the increase in temperature due to global warming is also very certain and can significantly impact drought and precipitation [87]. The integrated role of both precipitation and temperature can be further explored in unraveling the historic/future drought events and types, as well as in extreme precipitation events in the region that are not addressed in current work and thus will be explored in a separate study. Elevation-dependent increase was not so evident, except for the 95th percentile. This suggests that changes in P extremes over Pakistan on the daily scale may not be attributed to a specific season or months, as the mixed response from SqMK and linear trend suggest that both latitudinal and longitudinal precipitation extreme variability over the region is distinct.

Apart from the usual P systems, large scale circulation indices such as South Asian high, Himalayan forcing, and oceanic forcing could also be part of the shift [88,94,95]. Due to changes in global mean T, the current trend observed for the P extreme may further intensify due to strong land–ocean thermal gradient and can lead to more catastrophic events. The extreme P indices infer a general increasing trend in the extreme P events over Pakistan, and thus the associated risk may also increase. The increasing trends of these extreme P indices can be linked to global warming-induced changes in circulation, large scale indices, and land–ocean thermal gradient.

The findings of the study are based on the long-term observation records of in situ P and do not consider the direct influence of large-scale circulation and oceanic and associated drivers. These aspects will be covered in a separate study in more detail. Furthermore, the spatial distribution of the in situ stations across the country is also susceptible to substantial uncertainties such as the ability to capture trace P amount, rain shadow regions, and P bimodality due to two fronts during cold and warm seasons. These aspects may need to be considered in interpreting the localized trends and thus are well-acknowledged in the current study. Future studies should focus on the risk, exposure index, and associated remedies of such extreme precipitation indices in the region.

Author Contributions: Conceptualization, A.S.B. and G.W.; methodology, A.S.B. and W.U.; validation, D.F.T.H., S.U., and I.U.; formal analysis, A.S.B. and G.W.; resources, G.W.; data curation, I.K.N.; writing—original draft preparation, A.S.B.; writing—review and editing, I.K.N.; visualization, D.L.; supervision, G.W. and W.U.; funding acquisition, G.W. All authors have read and agreed to the published version of the manuscript.

Funding: This research was funded by the National Natural Science Foundation of China (41875094), National Key Research and Development Program of China (2017YFA0603701), and the Sino–German Cooperation Group Project (GZ1447).

Acknowledgments: We extend our special gratitude to the Pakistan Meteorological Department (PMD) for granting access to this essential dataset in accordance to their specific data use and citation policies.

Conflicts of Interest: The authors declare no conflict of interest.

References

1. IPCC. *Climate Change 2013: The Physical Science Basis*; Cambridge University Press: Cambridge, UK, 2013.
2. Zhang, Q.; Li, J.; Singh, V.P.; Xiao, M. Spatio-temporal relations between temperature and precipitation regimes: Implications for temperature-induced changes in the hydrological cycle. *Glob. Planet. Chang.* **2013**, *111*, 57–76. [[CrossRef](#)]
3. Sillmann, J.; Kharin, V.V.; Zwiers, F.W.; Zhang, X.; Bronaugh, D. Climate extremes indices in the CMIP5 multimodel ensemble : Part 2. Future climate projections. *J. Geophys. Res. Atmos.* **2013**, *118*, 2473–2493. [[CrossRef](#)]
4. Cheng, C.S.; Auld, H.; Li, Q.; Li, G. Possible impacts of climate change on extreme weather events at local scale in south-central Canada. *Clim. Chang.* **2012**, *112*, 963–979. [[CrossRef](#)]
5. Zhang, Q.; Gu, X.; Singh, V.P.; Kong, D.; Chen, X. Spatiotemporal behavior of floods and droughts and their impacts on agriculture in China. *Glob. Planet. Chang.* **2015**, *131*, 63–72. [[CrossRef](#)]
6. Moazami, S.; Golian, S.; Hong, Y.; Sheng, C.; Kavianpour, M.R. Comprehensive evaluation of four high-resolution satellite precipitation products under diverse climate conditions in Iran. *Hydrol. Sci. J.* **2016**, *61*, 420–440. [[CrossRef](#)]
7. Sun, Q.; Miao, C.; Duan, Q.; Wang, Y. Temperature and precipitation changes over the Loess Plateau between 1961 and 2011, based on high-density gauge observations. *Glob. Planet. Chang.* **2015**, *132*, 1–10. [[CrossRef](#)]
8. Berardy, A.; Chester, M.V. Climate change vulnerability in the food, energy, and water nexus: Concerns for agricultural production in Arizona and its urban export supply. *Environ. Res. Lett.* **2017**, *12*, 35004. [[CrossRef](#)]
9. Taxak, A.K.; Murumkar, A.R.; Arya, D.S. Long term spatial and temporal rainfall trends and homogeneity analysis in Wainganga basin, Central India. *Weather Clim. Extrem.* **2014**, *4*, 50–61. [[CrossRef](#)]
10. Herring, S.C.; Hoerling, M.P.; Kossin, J.P.; Peterson, T.C.; Stott, P.A. Explaining Extreme Events of 2014 from a Climate Perspective. *Bull. Am. Meteorol. Soc.* **2015**, *96*, S1–S172. [[CrossRef](#)]
11. Bintanja, R.; Selten, F.M. Future increases in Arctic precipitation linked to local evaporation and sea-ice retreat. *Nature* **2014**, *509*, 479–482. [[CrossRef](#)]
12. Kharin, V.V.; Zwiers, F.W.; Zhang, X.; Wehner, M. Changes in temperature and precipitation extremes in the CMIP5 ensemble. *Clim. Chang.* **2013**, *119*, 345–357. [[CrossRef](#)]
13. Scoccimarro, E.; Gualdi, S.; Bellucci, A.; Zampieri, M.; Navarra, A. Heavy precipitation events in a warmer climate: Results from CMIP5 models. *J. Clim.* **2013**, *26*, 7902–7911. [[CrossRef](#)]
14. Ahmad, I.; Tang, D.; Wang, T.; Wang, M.; Wagan, B. Precipitation Trends over Time Using Mann-Kendall and Spearman's rho Tests in Swat River Basin, Pakistan. *Adv. Meteorol.* **2015**, *43*, 431860. [[CrossRef](#)]
15. Xu, M.; Kang, S.; Wu, H.; Yuan, X. Detection of spatio-temporal variability of air temperature and precipitation based on long-term meteorological station observations over Tianshan Mountains, Central Asia. *Atmos. Res.* **2018**, *203*, 141–163. [[CrossRef](#)]
16. Karpouzou, D.; Kavalieratou, S.; Babajimopoulos, C. Trend analysis of precipitation data in Pieria Region (Greece). *Eur. Water* **2010**, *30*, 31–40.
17. Xu, W.; Ma, L.; Ma, M.; Zhang, H.; Yuan, W. Spatial-temporal variability of snow cover and depth in the Qinghai-Tibetan plateau. *J. Clim.* **2017**, *30*, 1521–1533. [[CrossRef](#)]
18. Rahman, G.; Rahman, A.; Sami, U.; Dawood, M. Spatial and temporal variation of rainfall and drought in Khyber Pakhtunkhwa Province of Pakistan during 1971–2015. *Arab. J. Geosci.* **2018**, *11*, 46. [[CrossRef](#)]
19. Ullah, W.; Nihei, T.; Nafees, M.; Zaman, R.; Ali, M. Understanding climate change vulnerability, adaptation and risk perceptions at household level in Khyber Pakhtunkhwa, Pakistan. *Int. J. Clim. Chang. Strateg. Manag.* **2018**, *10*, 359–378. [[CrossRef](#)]
20. You, Q.; Ren, G.Y.; Zhang, Y.Q.; Ren, Y.Y.; Sun, X.B.; Zhan, Y.J.; Shrestha, A.B.; Krishnan, R. An overview of studies of observed climate change in the Hindu Kush Himalayan (HKH) region. *Adv. Clim. Chang. Res.* **2017**, *8*, 141–147. [[CrossRef](#)]
21. Alexander, L.V.; Zhang, X.; Peterson, T.C.; Caesar, J.; Gleason, B.; Klein Tank, A.M.G.; Haylock, M.; Collins, D.; Trewin, B.; Rahimzadeh, F.; et al. Global observed changes in daily climate extremes of temperature and precipitation. *J. Geophys. Res. Atmos.* **2006**, *111*. [[CrossRef](#)]
22. Groisman, P.Y.; Knight, R.W.; Easterling, D.R.; Karl, T.R.; Hegerl, G.; Razuvaev, V.N. Trends in Intense Precipitation in the Climate Record. *J. Clim.* **2005**, *18*, 1326–1350. [[CrossRef](#)]

23. Ren, Y.Y.; Ren, G.Y.; Sun, X.B.; Shrestha, A.B.; You, Q.L.; Zhan, Y.J.; Rajbhandari, R.; Zhang, P.F.; Wen, K.M. Observed changes in surface air temperature and precipitation in the Hindu Kush Himalayan region over the last 100-plus years. *Adv. Clim. Chang. Res.* **2017**, *8*, 148–156. [[CrossRef](#)]
24. Sun, X.B.; Ren, G.Y.; Shrestha, A.B.; Ren, Y.Y.; You, Q.L.; Zhan, Y.J.; Xu, Y.; Rajbhandari, R. Changes in extreme temperature events over the Hindu Kush Himalaya during 1961–2015. *Adv. Clim. Chang. Res.* **2017**, *8*, 157–165. [[CrossRef](#)]
25. Sheikh, M.M.; Manzoor, N.; Ashraf, J.; Adnan, M.; Collins, D.; Hameed, S.; Manton, M.J.; Ahmed, A.U.; Baidya, S.K.; Borgaonkar, H.P.; et al. Trends in extreme daily rainfall and temperature indices over South Asia. *Int. J. Climatol.* **2015**, *35*, 1625–1637. [[CrossRef](#)]
26. Tank, K.A.M.G.; Peterson, C., T.; Quadir, D.A.; Dorji, S.; Zou, X.; Tang, H.; Santhosh, K.; Joshi, U.R.; Jaswal, A.K.; Kolli, R.K.; et al. Changes in daily temperature and precipitation extremes in central and south Asia. *J. Geophys. Res.* **2006**, *111*. [[CrossRef](#)]
27. Hartmann, H.; Buchanan, H. Trends in extreme precipitation events in the Indus River Basin and flooding in Pakistan. *Atmos. Ocean* **2014**, *52*, 77–91. [[CrossRef](#)]
28. Hu, Z.; Zhou, Q.; Chen, X.; Qian, C.; Wang, S.; Li, J. Variations and changes of annual precipitation in Central Asia over the last century. *Int. J. Climatol.* **2017**, *37*, 157–170. [[CrossRef](#)]
29. Hu, Z.; Hu, Q.; Zhang, C.; Chen, X.; Li, Q. Evaluation of Reanalysis, Spatially Interpolated and Satellite Remotely Sensed Precipitation Data Sets in Central Asia. *J. Geophys. Res. Atmos.* **2016**, *121*, 5648–5663. [[CrossRef](#)]
30. Hu, Z.; Li, Q.; Chen, X.; Teng, Z.; Chen, C.; Yin, G.; Zhang, Y. Climate changes in temperature and precipitation extremes in an alpine grassland of Central Asia. *Theor. Appl. Climatol.* **2016**, *126*, 519–531. [[CrossRef](#)]
31. Moberg, A.; Jones, P.D.; Lister, D.; Walther, A.; Brunet, M.; Jacobeit, J.; Alexander, L.V.; Della-Marta, P.M.; Luterbacher, J.; Yiou, P.; et al. Indices for daily temperature and precipitation extremes in Europe analyzed for the period 1901–2000. *J. Geophys. Res. Atmos.* **2006**, *111*. [[CrossRef](#)]
32. Tank, K.A.M.G.; Können, G.P. Trends in Indices of daily temperature and precipitation extremes in Europe, 1946–1999. *J. Clim.* **2003**, *16*, 3665–3680. [[CrossRef](#)]
33. Donat, M.G.; Peterson, T.C.; Brunet, M.; King, A.D.; Almazroui, M.; Kolli, R.K.; Boucherf, D.; Al-Mulla, A.Y.; Nour, A.Y.; Aly, A.A.; et al. Changes in extreme temperature and precipitation in the Arab region: Long-term trends and variability related to ENSO and NAO. *Int. J. Climatol.* **2014**, *34*, 581–592. [[CrossRef](#)]
34. Almazroui, M.; Islam, M.N.; Dambul, R.; Jones, P.D. Trends of temperature extremes in Saudi Arabia. *Int. J. Climatol.* **2014**, *34*, 808–826. [[CrossRef](#)]
35. Zhou, B.; Xu, Y.; Wu, J.; Dong, S.; Shi, Y. Changes in temperature and precipitation extreme indices over China: Analysis of a high-resolution grid dataset. *Int. J. Climatol.* **2016**, *36*, 1051–1066. [[CrossRef](#)]
36. Sun, W.; Mu, X.; Song, X.; Wu, D.; Cheng, A.; Qiu, B. Changes in extreme temperature and precipitation events in the Loess Plateau (China) during 1960–2013 under global warming. *Atmos. Res.* **2016**, *168*, 33–48. [[CrossRef](#)]
37. You, Q.; Kang, S.; Aguilar, E.; Pepin, N.; Flugel, W.A.; Yan, Y.; Xu, Y.; Zhang, Y.; Huang, J. Changes in daily climate extremes in China and their connection to the large scale atmospheric circulation during 1961–2003. *Clim. Dyn.* **2011**, *36*, 2399–2417. [[CrossRef](#)]
38. Li, Z.; He, Y.; Wang, P.; Theakstone, W.H.; An, W.; Wang, X.; Lu, A.; Zhang, W.; Cao, W. Changes of daily climate extremes in southwestern China during 1961–2008. *Glob. Planet. Chang.* **2012**, *80–81*, 255–272.
39. Shahid, S. Trends in extreme rainfall events of Bangladesh. *Theor. Appl. Climatol.* **2011**, *104*, 489–499. [[CrossRef](#)]
40. Shahid, S.; Wang, X.J.; Harun, S.B.; Shamsudin, S.B.; Ismail, T.; Minhans, A. Climate variability and changes in the major cities of Bangladesh: Observations, possible impacts and adaptation. *Reg. Environ. Chang.* **2016**, *16*, 459–471. [[CrossRef](#)]
41. Endo, N.; Matsumoto, J.; Hayashi, T.; Terao, T.; Murata, F.; Kiguchi, M.; Yamane, Y.; Alam, S. Trends in Precipitation Characteristics in Bangladesh from 1950 to 2008. *SOLA* **2015**, *11*, 7–11. [[CrossRef](#)]
42. Deshpande, N.R.; Kothawale, D.R.; Kulkarni, A. Changes in climate extremes over major river basins of India. *Int. J. Climatol.* **2016**, *36*, 4548–4559. [[CrossRef](#)]
43. Ullah, S.; You, Q.; Ali, A.; Ullah, W.; Jan, M.A.; Zhang, Y.; Xie, W.; Xie, X. Observed changes in maximum and minimum temperatures over China-Pakistan economic corridor during 1980–2016. *Atmos. Res.* **2019**, *216*, 37–51. [[CrossRef](#)]

44. Ashiq, M.W.; Zhao, C.; Ni, J.; Akhtar, M. GIS-based high-resolution spatial interpolation of precipitation in mountain-plain areas of Upper Pakistan for regional climate change impact studies. *Theor. Appl. Climatol.* **2010**, *99*, 239–253. [[CrossRef](#)]
45. Hussain, M.S.; Lee, S. The regional and the seasonal variability of extreme precipitation trends in Pakistan. *Asia-Pac. J. Atmos. Sci.* **2013**, *49*, 421–441. [[CrossRef](#)]
46. Ullah, S.; You, Q.; Ullah, W.; Ali, A. Observed changes in precipitation in China-Pakistan economic corridor during 1980–2016. *Atmos. Res.* **2018**, *210*, 1–14. [[CrossRef](#)]
47. Kreft, S.; Eckstein, D.; Junghans, L.; Kerestan, C.; Hagen, U. *Global Climate Risk Index. Who Suffers Most from Extreme Weather Events? Weather-related Loss Events in 2013 and 1994 to 2013*; German Watch: Bonn, Germany, 2015.
48. Zhan, Y.J.; Ren, G.Y.; Shrestha, A.B.; Rajbhandari, R.; Ren, Y.Y.; Sanjay, J.; Xu, Y.; Sun, X.B.; You, Q.L.; Wang, S. Changes in extreme precipitation events over the Hindu Kush Himalayan region during 1961–2012. *Adv. Clim. Chang. Res.* **2017**, *8*, 166–175. [[CrossRef](#)]
49. Zahid, M.; Rasul, G. Frequency of Extreme Temperature & Precipitation Events in Pakistan 1965–2009. *Sci. Int* **2011**, *23*, 313–319.
50. Abbas, F.; Ahmad, A.; Safeeq, M.; Ali, S.; Saleem, F.; Hammad, H.M.; Farhad, W. Changes in precipitation extremes over arid to semiarid and subhumid Punjab, Pakistan. *Theor. Appl. Climatol.* **2014**, *116*, 671–680. [[CrossRef](#)]
51. Abbas, F.; Sarwar, N.; Ibrahim, M.; Adrees, M.; Ali, S.; Saleem, F.; Hammad, H.M. Patterns of climate extremes in the coastal and highland regions of Balochistan—Pakistan. *Earth Interact.* **2018**, *22*. [[CrossRef](#)]
52. Abbas, F.; Rehman, I.; Adrees, M.; Ibrahim, M.; Saleem, F.; Ali, S.; Rizwan, M.; Salik, M.R. Prevailing trends of climatic extremes across Indus-Delta of Sindh-Pakistan. *Theor. Appl. Climatol.* **2018**, *131*, 1101–1117. [[CrossRef](#)]
53. Hassan, S.A.; Ansari, M.R.K. Hydro-climatic aspects of Indus River flow propagation. *Arab. J. Geosci.* **2015**, *8*, 10977–10982. [[CrossRef](#)]
54. Mahmood, R.; Jia, S. Assessment of Impacts of Climate Change on the Water Resources of the Transboundary Jhelum River Basin of Pakistan and India. *Water* **2016**, *8*, 246. [[CrossRef](#)]
55. Xie, H.; Ringler, C.; Zhu, T.; Waqas, A. Droughts in Pakistan: A spatiotemporal variability analysis using the Standardized Precipitation Index. *Water Int.* **2013**, *38*, 620–631. [[CrossRef](#)]
56. Rahman, A.u.; Khan, A.N. Analysis of flood causes and associated socio-economic damages in the Hindukush region. *Nat. Hazards* **2011**, *59*, 1239. [[CrossRef](#)]
57. Gadiwala, M.S.; Burke, F. Climate Change and Precipitation in Pakistan—A Meteorological Prospect. *Int. Econ. Environ. Geol.* **2013**, *4*, 10–15.
58. Arshad, M.; Kächele, H.; Krupnik, T.J.; Amjath-Babu, T.S.; Aravindakshan, S.; Abbas, A.; Mehmood, Y.; Müller, K. Climate variability, farmland value, and farmers’ perceptions of climate change: Implications for adaptation in rural Pakistan. *Int. J. Sustain. Dev. World Ecol.* **2017**, *24*, 532–544. [[CrossRef](#)]
59. Ullah, W.; Wang, G.; Ali, G.; Tawia Hagan, D.; Bhatti, A.S.; Lou, D. Comparing Multiple Precipitation Products against In-Situ Observations over Different Climate Regions of Pakistan. *Remote Sens.* **2019**, *11*, 628. [[CrossRef](#)]
60. Ullah, S.; You, Q.; Ullah, W.; Hagan, F.D.T.; Ali, A.; Ali, G.; Zhang, Y.; Jan, M.A.; Bhatti, A.S.; Xie, W. Daytime and nighttime heat wave characteristics based on multiple indices over the China—Pakistan economic corridor. *Clim. Dyn.* **2019**, *53*, 6329–6349. [[CrossRef](#)]
61. Iqbal, M.F.; Athar, H. Validation of satellite based precipitation over diverse topography of Pakistan. *Atmos. Res.* **2018**, *201*, 247–260. [[CrossRef](#)]
62. Waqas, A.; Athar, H. Spatiotemporal variability in daily observed precipitation and its relationship with snow cover of Hindukush, Karakoram and Himalaya region in northern Pakistan. *Atmos. Res.* **2019**, *228*, 196–205. [[CrossRef](#)]
63. Ullah, S.; You, Q.; Ullah, W.; Ali, A.; Xie, W.; Xie, X. Observed Changes in Temperature Extremes over China-Pakistan Economic Corridor during 1980-2016. *Int. J. Climatol.* **2018**, *39*, 1457–1475. [[CrossRef](#)]
64. Ali, S.; Eum, H.I.; Cho, J.; Dan, L.; Khan, F.; Dairaku, K.; Shrestha, M.L.; Hwang, S.; Nasim, W.; Khan, I.A.; et al. Assessment of climate extremes in future projections downscaled by multiple statistical downscaling methods over Pakistan. *Atmos. Res.* **2019**, *222*, 114–133. [[CrossRef](#)]

65. Trenberth, K.E.; Fasullo, J.T. Climate extremes and climate change: The Russian heat wave and other climate extremes of 2010. *J. Geophys. Res. Atmos.* **2012**, *117*. [[CrossRef](#)]
66. Thom, H.C.S. Some methods of climatological analysis. *WMO Tech.* **1966**, *81*, 55.
67. Ribeiro, S.; Caineta, J.; Costa, A.C. Review and discussion of homogenisation methods for climate data. *Phys. Chem. Earth* **2016**, *94*, 167–179. [[CrossRef](#)]
68. Kang, H.M.; Yusof, F. Homogeneity Tests on Daily Rainfall Series in Peninsular Malaysia. *Int. J. Contemp. Math. Sci.* **2012**, *7*, 9–22.
69. Gonzalez-Rouco, J.F.; Jimenez, J.L.; Quesada, V.; Valero, F. Quality Control and Homogeneity of Precipitation Data in the Southwest of Europe. *J. Clim.* **2001**, *14*, 964–978. [[CrossRef](#)]
70. Ongoma, V.; Chen, H.; Gao, C.; Nyongesa, A.M.; Polong, F. Future changes in climate extremes over Equatorial East Africa based on CMIP5 multimodel ensemble. *Nat. Hazards* **2018**, *90*, 901–920. [[CrossRef](#)]
71. Zhang, X.; Alexander, L.; Hegerl, G.C.; Jones, P.; Tank, A.K.; Peterson, T.C.; Trewin, B.; Zwiers, F.W. Indices for monitoring changes in extremes based on daily temperature and precipitation data. *Wiley Interdiscip. Rev. Clim. Chang.* **2011**, *2*, 851–870. [[CrossRef](#)]
72. Mann, H.B. Nonparametric Tests against Trend. *Econometrica* **1945**, *13*, 245–259. [[CrossRef](#)]
73. Kendall, M.G. *Rank Correlation Methods*, 2nd ed.; Hafner Publishing Co.: Oxford, UK, 1955.
74. Sen, P.K. Estimates of the Regression Coefficient Based on Kendall's Tau. *J. Am. Stat. Assoc.* **1968**, *63*, 1379–1389. [[CrossRef](#)]
75. Anjum, R.; He, X.; Tanoli, J.I.; Raza, S.T. Contemporary temperature fluctuation in urban areas of Pakistan. *Atmosphere* **2017**, *8*, 12. [[CrossRef](#)]
76. Qiu, J.; Gao, Q.; Wang, S.; Su, Z. Comparison of temporal trends from multiple soil moisture data sets and precipitation: The implication of irrigation on regional soil moisture trend. *Int. J. Appl. Earth Obs. Geoinf.* **2016**, *48*, 17–27. [[CrossRef](#)]
77. Jiang, R.; Wang, Y.; Xie, J.; Zhao, Y.; Li, F.; Wang, X. Assessment of extreme precipitation events and their teleconnections to El Niño Southern Oscillation, a case study in the Wei River Basin of China. *Atmos. Res.* **2019**, *218*, 372–384. [[CrossRef](#)]
78. Iqbal, M.A.; Penas, A.; Cano-Ortiz, A.; Kersebaum, K.C.; Herrero, L.; del Río, S. Analysis of recent changes in maximum and minimum temperatures in Pakistan. *Atmos. Res.* **2016**, *168*, 234–249. [[CrossRef](#)]
79. Wen, X.; Wu, X.; Gao, M. Spatiotemporal variability of temperature and precipitation in Gansu Province (Northwest China) during 1951–2015. *Atmos. Res.* **2017**, *197*, 132–149. [[CrossRef](#)]
80. Martinez, C.J.; Maleski, J.J.; Miller, M.F. Trends in precipitation and temperature in Florida, USA. *J. Hydrol.* **2012**, *452–453*, 259–281. [[CrossRef](#)]
81. Rahman, A.; Dawood, M. Spatio-statistical analysis of temperature fluctuation using Mann–Kendall and Sen's slope approach. *Clim. Dyn.* **2017**, *48*, 783–797. [[CrossRef](#)]
82. Wang, G.; Gong, T.; Lu, J.; Lou, D.; Hagan, D.F.T.; Chen, T. On the long-term changes of drought over China (1948–2012) from different methods of potential evapotranspiration estimations. *Int. J. Climatol.* **2018**, *38*, 2954–2966. [[CrossRef](#)]
83. Ongoma, V.; Chen, H.; Omony, G.W. Variability of extreme weather events over the equatorial East Africa, a case study of rainfall in Kenya and Uganda. *Theor. Appl. Climatol.* **2018**, *131*, 295–308. [[CrossRef](#)]
84. Sneyers, S. *On the Statistical Analysis of Series of Observations*; Technical Note No. 143, WMO No. 725 415; Secretariat of the World Meteorological Organization: Geneva, Switzerland, 1990.
85. Ahmed, K.; Shahid, S.; Wang, X.; Nawaz, N.; Khan, N. Spatiotemporal changes in aridity of Pakistan during 1901–2016. *Hydrol. Earth Syst. Sci.* **2019**, *23*, 3081–3096. [[CrossRef](#)]
86. Galarneau, T.J.; Hamill, T.M.; Dole, R.M.; Perlwitz, J. A Multiscale Analysis of the Extreme Weather Events over Western Russia and Northern Pakistan during July 2010. *Mon. Weather Rev.* **2012**, *140*, 1639–1664. [[CrossRef](#)]
87. Ahmed, K.; Shahid, S.; Nawaz, N. Impacts of climate variability and change on seasonal drought characteristics of Pakistan. *Atmos. Res.* **2018**, *241*, 364–374. [[CrossRef](#)]
88. Rasmussen, K.L.; Hill, A.J.; Toma, V.E.; Zuluaga, M.D.; Webster, P.J.; Houze, R.A. Multiscale analysis of three consecutive years of anomalous flooding in Pakistan. *Q. J. R. Meteorol. Soc.* **2015**, *141*, 1259–1276. [[CrossRef](#)]
89. Iqbal, M.F.; Athar, H. Variability, trends, and teleconnections of observed precipitation over Pakistan. *Theor. Appl. Climatol.* **2017**, *134*, 613–632. [[CrossRef](#)]

90. Dimri, A.P.; Niyogi, D.; Barros, A.P.; Ridley, J.; Mohanty, U.C.; Yasunari, T.; Sikka, D.R. Western Disturbances: A review. *Rev. Geophys.* **2015**, *53*, 225–246. [[CrossRef](#)]
91. Haider, S.; Adnan, S. Classification and Assessment of Aridity Over Pakistan Provinces (1960–2009). *Int. J. Environ.* **2014**, *3*, 24–35. [[CrossRef](#)]
92. Chen, F.; Chen, J.; Huang, W.; Chen, S.; Huang, X.; Jin, L.; Jia, J.; Zhang, X.; An, C.; Zhang, J.; et al. Westerlies Asia and monsoonal Asia: Spatiotemporal differences in climate change and possible mechanisms on decadal to sub-orbital timescales. *Earth Sci. Rev.* **2019**, *192*, 337–354. [[CrossRef](#)]
93. Kotlia, B.S.; Singh, A.K.; Joshi, L.M.; Dhaila, B.S. Precipitation variability in the Indian Central Himalaya during last ca. 4000 years inferred from a speleothem record: Impact of Indian Summer Monsoon (ISM) and Westerlies. *Quat. Int.* **2015**, *371*, 244–253. [[CrossRef](#)]
94. Latif, M.; Hannachi, A.; Syed, F.S. Analysis of rainfall trends over Indo-Pakistan summer monsoon and related dynamics based on CMIP5 climate model simulations. *Int. J. Climatol.* **2018**, *38*, 577–595. [[CrossRef](#)]
95. Fowler, H.J.; Archer, D.R. Conflicting signals of climatic change in the upper Indus Basin. *J. Clim.* **2006**, *19*, 4276–4293. [[CrossRef](#)]



© 2020 by the authors. Licensee MDPI, Basel, Switzerland. This article is an open access article distributed under the terms and conditions of the Creative Commons Attribution (CC BY) license (<http://creativecommons.org/licenses/by/4.0/>).